Journal of Alloys and Compounds 509 (2011) 435–439

Contents lists available at ScienceDirect

Journal of Alloys and Compounds

journal homepage: www.elsevier.com/locate/jallcom

Variation in structural and dielectric properties of co-precipitated nanoparticles strontium ferrites due to value of pH

M. Anis-ur-Rehman*, G. Asghar

Applied Thermal Physics Laboratory, Department of Physics, COMSATS Institute of Information Technology, Islamabad 44000, Pakistan

ARTICLE INFO

Article history:
Received 28 February 2010
Received in revised form 9 September 2010
Accepted 9 September 2010
Available online 22 September 2010

Keywords:
Hard magnets
Electrical properties
Grain boundaries
Dielectric
Hopping electron
Hexagonal ferrite

ABSTRACT

Nanoparticles of strontium ferrites with nominal composition $SrFe_{12}O_{19}$ were prepared by co-precipitation method, by decreasing pH from 13 to 8 with a regular step of 1. The secondary phase of α-Fe_2O_3 was increased with the decrease in pH. The crystallite size estimated from X-rays diffraction data was in the range 52–70 nm, which is much smaller than that already reported. Most of the particles formed had hexagonal structure, as observed by the scanning electron microscopy. Particle size and dielectric loss were increased where as dc electrical resistivity and dielectric constant were decreased with decrease in pH. The results show that the material synthesized with higher pH is phase pure and is potentially more suitable for high frequency applications.

1. Introduction

Ferrites are ferrimagnetic ceramic materials that can be magnetized to produce large magnetic flux densities in response to small applied magnetic forces. They are considered better than other magnetic materials because they have high electrical resistivity and low eddy current losses [1]. These are one of the most significant dielectric materials whose properties depend upon synthesis conditions, composition, sintering temperature and grain size [2–4]. Among these materials, M-type hexa-ferrites $MFe_{12}O_{19}$ (M = Ba, Sr, Pb) have been a subject of continuous interest for several decades due to the fact that these compounds have been the work horse of the permanent magnet market [5,6]. Prepared $SrFe_{12}O_{19}$ can be used as magnetic fillers in microwave absorber components [7–9]. These materials can also find their applications in magnetic recording media, electronic devices, medicine and magneto-optical recording [10–14].

For microwave applications, the dielectric properties such as dielectric constant and dielectric loss are very important as the dielectric constant affects the thickness of microwave absorbing layer and the dielectric loss factor ($\tan\delta$) of a material determines dissipation of the electrical energy. This dissipation may be due to electrical conduction, dielectric relaxation, dielectric resonance and loss from non-linear processes [15]. High performance devices require low dielectric loss ($\tan\delta$) because the lower it is the higher the efficiency and lower the noise. The porosity of the material also increases the dielectric loss ($\tan\delta$) and that may be due to absorption of humidity by the pores of that material [16].

M-type hexa-ferrites are highly resistive. The electronic conduction at high temperature in ferrites is mainly due to hopping of electrons between ions of the same element present in more than one valence state, distributed randomly over crystallographic equivalent lattice sites [17]. The wet chemical method provides better control on particle size distribution and chemical homogeneity [18–20]. In co-precipitation method, pH plays very important role. In the present work a comparative study of effect of pH on structural and dielectric properties of strontium hexa-ferrites synthesized by co-precipitation method is given.

2. Experimental

Strontium hexa-ferrite nano particles with different pH values were prepared by co-precipitation method. It provides better control on structural parameters at nano scale. The chemicals used for the synthesis of samples were $Sr(NO_3)_2$ and $Fe(NO_3)_3{\cdot}9H_2O$. The salts were dissolved in de-ionized water. The solution of both of these precursors with molar ratio (Fe/Sr = 11) was prepared. This solution was heated along with continuous stirring on hot plate. When temperature of solution was reached to 70 °C, solution of NaOH was added until required pH was achieved. pH of the samples was varied from 13 to 08. The aqueous solution was stirred for 1 h to get fine homogeneity. The solution was washed for four times with de-ionized water and then dried in an oven at 105 °C. The dry precursors were ground well and then their pellets were formed using a pressure of 75 kg m^{-2}. These pellets were sintered in a box furnace for 1 h at 925 °C. The phase formation was studied by powder X-rays diffraction (XRD) using Cu-Kα (λ = 1.5406 Å). Structural morphology was studied by scanning electron microscope (SEM). Effect of temperature on resistance

* Corresponding author. Tel.: +92 321 5163059.
E-mail address: marehman@comsats.edu.pk (M. Anis-ur-Rehman).

0925-8388/$ – see front matter © 2010 Elsevier B.V. All rights reserved.
doi:10.1016/j.jallcom.2010.09.050

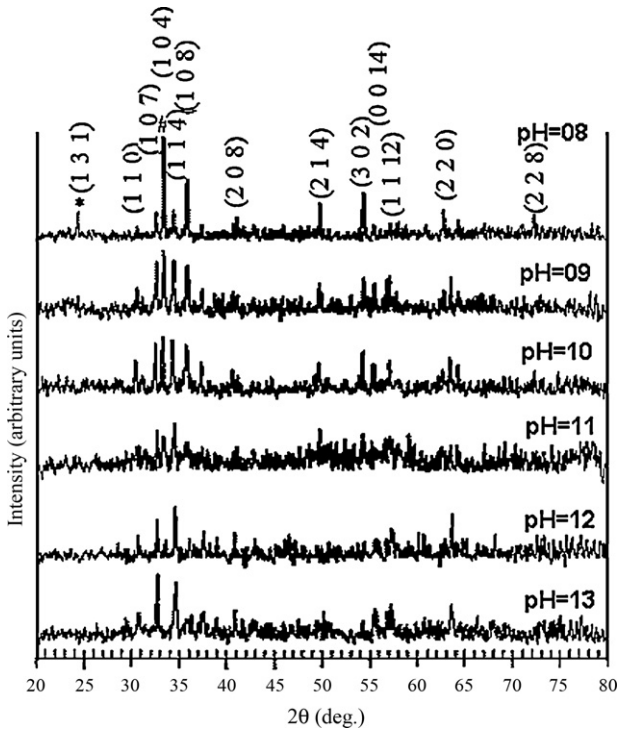

Fig. 1. Indexed patterns of XRD of samples of $SrFe_{12}O_{19}$ for different values of pH (* - $SrFe_2O_4$, # - α-Fe_2O_3).

and drift mobility of charge carriers were investigated. Apparatus to study the effect of temperature on resistance was designed and assembled in the laboratory. The dielectric constant (ε') and dielectric loss ($\tan\delta$) were measured in the frequency range of 1 kHz to 3 MHz using precision component analyzer.

3. Results and discussion

3.1. Structural analysis

Structural analysis was done by using XRD patterns and SEM. Fig. 1 shows indexed XRD patterns of the strontium hexa-ferrite samples for the different pH values, synthesized by the co-precipitation method. All the peaks were indexed by comparing with ICSD 01-080-1197, 00-048-0156 and 00-002-0919. Indexed XRD patterns showed that as pH was decreased from 13, extra phase of α-Fe_2O_3 started appearing and increased with the further decrease in pH. Parameters such as crystallite size (D), lattice parameters a (Å) and c (Å), cell volume (V) and X-ray density (ρ_x) were calculated from indexed XRD patterns and are given in Table 1. The crystallite size (D) was calculated by using Scherer's formula [21]. The crystallite size was in range 52–70 nm which is much smaller than that already reported [22]. This may be due to difference in molarities of solution. X-ray density (ρ_x) and bulk density (ρ_m) were calculated by using Eqs. (1) and (2) respectively.

$$\rho_x = \frac{\text{Number of formula units/unit cell} \times M_m}{VN_A} \quad (1)$$

where M_m is molecular mass, V is volume of unit cell, N_A is Avogadro's number.

$$\rho_m = \frac{m}{v} \quad (2)$$

where m is mass of pellet and v is volume of pellet.

Structural morphology was studied by SEM and is given in Fig. 2. The micrographs of pH varying samples of strontium hexa-ferrite showed that the particle size increased with the decrease in pH and most of the particles had hexagonal structure with diameter in the range of 0.4–3.5 μm. As the pH increased, the rate of nucleation sites formation increased which resulted in decrease in agglomeration. Distribution in particle size was also increased with the decrease in pH. This behavior is different as reported by Hessien et al. [21].

3.2. Electrical properties

The electrical properties of the ferrites depend upon particle size, chemical composition, synthesis technique and sintering temperature. Octahedral sites of hexa-ferrites are mainly responsible for electrical conduction. It is the number of ferrous ions on the octahedral sites that play a dominant role in the process of conduction as well as dielectric polarization [23]. According to the band theory, the temperature dependence of conductivity is mainly due to the variation in the charge carrier concentration with temperature. According to the hopping model, the change in their mobility with temperature is considered to lead to the conduction current by jumping or hopping from one iron ion to the next [24]. The conduction at room temperature is because of impurities and at high temperature it is due to polaron hopping explained by Verwey's hopping mechanism. According to Verwey, the electronic conduction in ferrites is mainly due to hopping of electrons between ions of the same element present in more than one valence state, distributed randomly over crystallographic equivalent lattice sites [17]. The crystal structure of ferrites shows that the cations either in tetrahedral or octahedral sites are surrounded by oxygen anions and to a first approximation can be treated as isolated from each other. Thus the localized electron model is more appropriate to discuss the conduction mechanism in ferrite rather than the band model [23]. M-type hexa-ferrites belong to $P6_3/mmc$ space group and crystallize in a hexagonal structure containing 64 ions per unit cell on 11 different symmetry sites. The 24 Fe atoms are distributed over five distinct sites: three octahedral (B) sites (12k, 2a, and $4f_2$), one tetrahedral (A) ($4f_1$) site and one bipyramidal (C) site (2b). The magnetic structure is ferrimagnetic with five different sublattices: three parallel (12k, 2a, and 2b) and two antiparallel ($4f_1$ and $4f_2$) [15,16]. Two tetrahedral sites are adjacent to each other and for these two only one metal ion is available. This metal ion now occupies position halfway between them, amidst the three oxygen ions. The distance between two metal ions at (B) site is smaller than

Table 1
Lattice constants a (Å) and c (Å), crystallite size (D), cell volume (V), X-ray density (ρ_x), bulk density (ρ_m), % age α-Fe_2O_3 and particle size. Standard deviations are also mentioned.

	pH = 13	pH = 12	pH = 11	pH = 10	pH = 09	pH = 08
Lattice constant a (Å) c (Å)	5.82(5)23.12(4)	5.88(2)23.00(6)	5.86(3)22.84(9)	5.87(2)23.03(4)	5.89(2)23.04(2)	5.86(3)23.06(4)
Crystallite size, D_{av} (nm)	62	68	65	59	69	59
Volume, V (Å^3)	678(6)	688(7)	685(9)	686(7)	689(5)	686(9)
X-ray density, ρ_x (g/cm^3)	5.20	5.13	5.15	5.13	5.12	5.15
Bulk density, ρ_m (g/cm^3)	3.27	3.18	3.39	3.53	3.29	3.63
% age of α-Fe_2O_3	0	5	10	16	20	24
Particle size (μm)	0.6–0.9	0.5–1.2	0.5–1.5	0.5–2.0	0.8–3.0	0.4–3.5

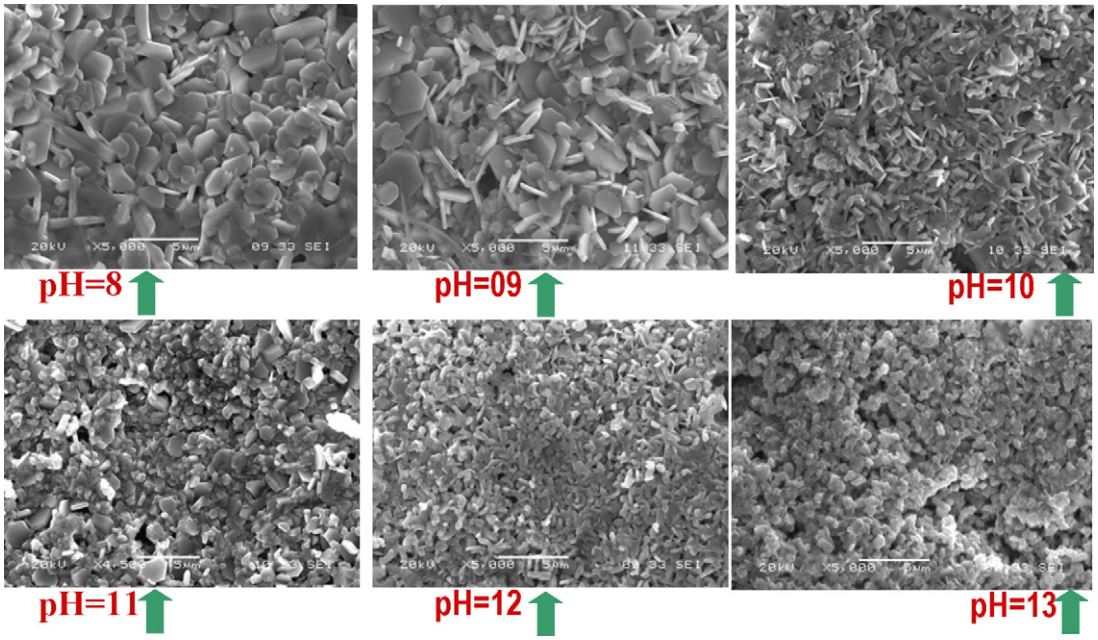

Fig. 2. SEM micrographs of the sintered samples of $SrFe_{12}O_{19}$ for different values of pH.

the distance between a metal ion at (B) site and another metal ion at (A) site. The electron hopping between (A) and (B) sites under normal conditions therefore has a very small probability compared with that for (B)–(B) hopping. Hopping between (A)–(A) sites does not exist for the simple reason that there are only Fe^{3+} ions at the (A) site and any Fe^{2+} ions formed during processing preferentially occupy (B) sites only. The hopping probability depends upon the separation between the ions involved and the activation energy [23]. The temperature dependent dc electrical resistivity was measured up to 703 K. Fig. 3(a) clearly indicated that resistivity of the samples was decreased with the increase in temperature so M-type ferrites behave like semiconductors [25]. This was due to the fact that the kinetic energy of the electrons was increased with the rise in temperature. The rate of hopping of electrons from one octahedral site to the other was increased and hence resistivity was decreased. Moreover the decrease in resistivity with the decrease in pH was because of variation in particle size. As the particle size was increased, the number of grain boundaries were decreased which acts as resistive medium and hence resistivity was decreased. Activation energy was calculated from the slope of the linear plots of ln ρ versus reciprocal of the temperature using Arrhenius relation [26] shown in Fig. 3(a).

Arrhenius relation is given by

$$\rho = \rho_0 \exp^{E_a/k_B T} \tag{3}$$

where ρ is resistivity at temperature T, ρ_o is resistivity at 0 K, E_a is the activation energy and k_B is the Boltzmann's constant.

The drift mobility was calculated using the equation

$$\mu = \frac{1}{ne\rho} \tag{4}$$

where e is charge of electron, ρ is the resistivity at temperature T and n is the concentration of charge carriers given by the equation

$$n = \frac{N_A D_B P_{Fe}}{M} \tag{5}$$

where N_A is the Avogadro's number, D_B is the bulk density, P_{Fe} is the number of iron atoms and M is the molecular weight of the chemical formula.

Effect of temperature on drift mobility has been shown in Fig. 3(b). The graph of drift mobility verses temperature showed that it was increased with the rise in temperature. This was because the charge carriers started moving easily from one lattice site to another due to the increase in temperature.

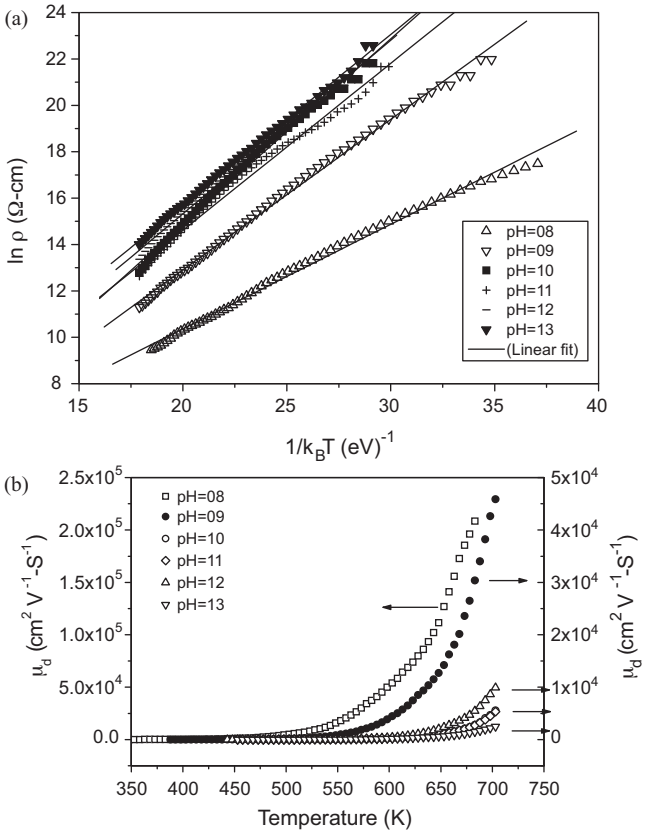

Fig. 3. Plot of (a) ln of dc electrical resistivity, ρ and (b) drift mobility, μ_d of samples of $SrFe_{12}O_{19}$ for different values of pH.

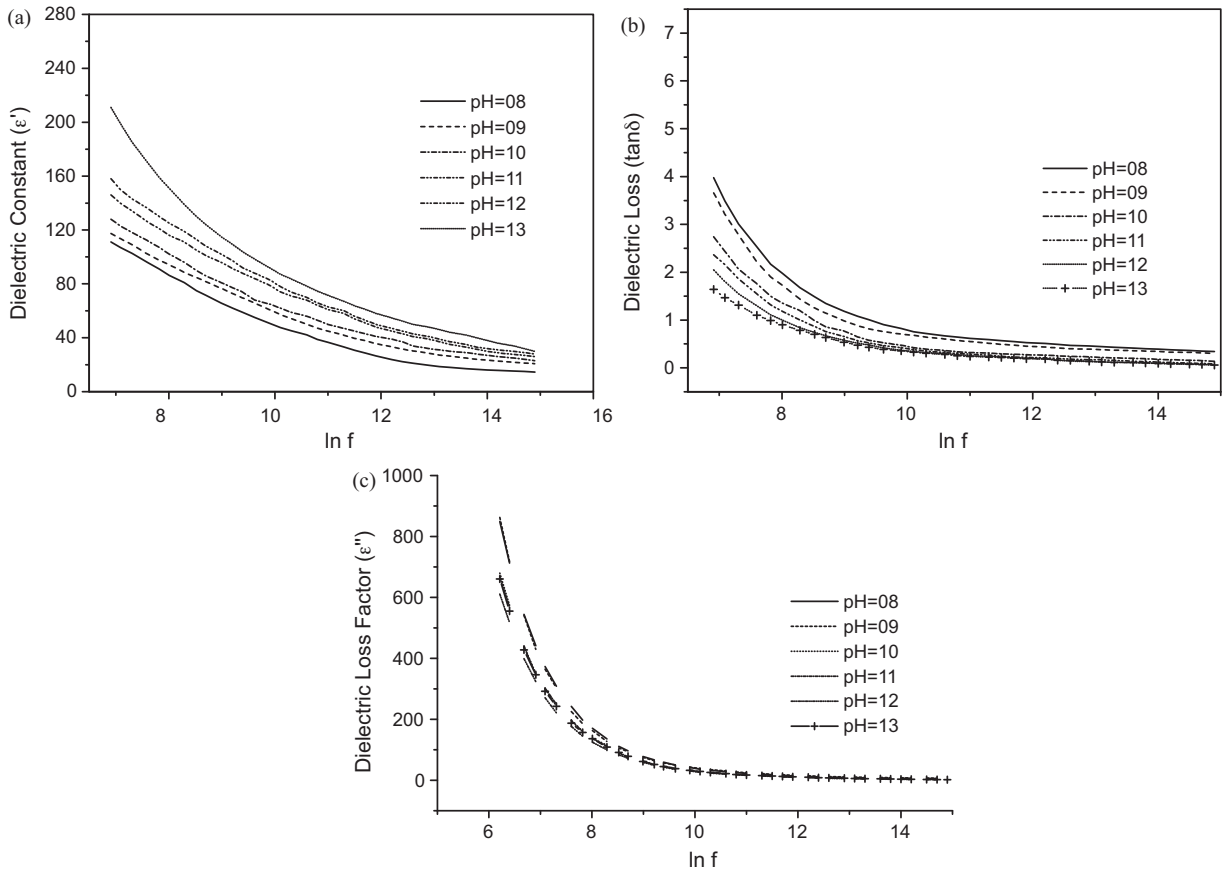

Fig. 4. The plot of (a) dielectric constant (ε'), (b) dielectric loss ($\tan\delta$) and dielectric loss factor (ε'') as a function of log of frequency of samples of $SrFe_{12}O_{19}$ for different values of pH.

3.3. Dielectric properties

The dielectric constant (ε') of a material determines the relative speed that an electromagnetic signal can travel in that material. When microwaves enter in a dielectric material, their speed decreases by a factor nearly equal to the square root of the dielectric constant (ε'). This could be explained by Maxwell–Wagner model [27]. According to Maxwell–Wagner model, the dielectric structure of ferrites consists two layers. First layer consists of large number of grains that acts as conducting layer at higher frequencies and the other layer consists of grain boundaries that act as highly resistive medium at lower frequencies. The polarization in ferrites is similar to the conduction process i.e. by electron exchange between Fe^{2+} and Fe^{3+} ions [28]. The decrease in dielectric constant with the increase in frequency is because of charge polarization. The charge polarization takes place by hopping of electron between Fe^{2+} and Fe^{3+} ions. As the frequency of the applied electric field increases, it becomes more difficult for the electron to hope from Fe^{2+} and Fe^{3+} ions with the alternating frequency, the net displacement of charge in one direction decreases and hence dielectric constant decreases. It is observed that at relatively lower frequencies the values of dielectric constant is high. It may be because of moisture, voids, dislocations, density and impurities [29]. Fig. 4(a) shows that the dielectric constant (ε') depends upon the pH value of the samples. It decreases with the decrease in pH and this effect is prominent at low frequencies. This is because of the grain size and secondary phase (α-Fe_2O_3) which increases with the decrease in pH. The concentration of Fe^{2+} ions decreases due to which the polarization decreases and hence dielectric constant decreases [30]. This could also be explained by Koops [31] model according to which the dielectric constant at low frequency is because of grain boundaries. These grain boundaries acts as high resistive medium and thus contribute to high dielectric constant. As the decrease in pH results in increase in the grain size and decrease in grain boundaries and hence decrease in dielectric constant [13].

Fig. 4(b) shows that the dielectric loss ($\tan\delta$) for all samples is greater at low frequencies and decreases rapidly with the increase in frequency. At lower frequencies, high dielectric loss may be because of impurities, crystal defects and moisture. The decrease in dielectric loss with the increase in frequency is because of charge polarization. As the frequency of the applied electric field increases, the polarization lags the alternating field. The net displacement

Table 2
Dielectric loss ($\tan\delta$), dielectric constant (ε'), dc electrical resistivity (ρ) and drift mobility (μ_d) of samples of $SrFe_{12}O_{19}$ for different values of pH.

	pH = 13	pH = 12	pH = 11	pH = 10	pH = 09	pH = 08
$\tan\delta$ (1 kHz)	1.64	2.05	2.36	2.74	3.65	4
$\tan\delta$ (3 MHz)	0.06	0.06	0.08	0.14	0.3	0.34
ε' (1 kHz)	211	158	146	128	117	111
ε' (3 MHz)	30	28	26	23	20.8	14.6
ρ (Ω-cm) at 603 K	1.66×10^7	1.20×10^7	5.90×10^6	1.12×10^7	8.28×10^5	4.96×10^4
μ_d ($V^{-1}\,S^{-1}\,cm^2$) at 603 K	1.79×10^{-11}	2.76×10^{-11}	5.15×10^{-11}	2.36×10^{-11}	5.41×10^{-9}	5.41×10^{-9}

of charge in one direction decreases and hence dielectric loss decreases. Fig. 4(b) also shows that at lower frequencies, dielectric losses increases with the decrease in pH and becomes nearly uniform at higher frequencies. This is because of conduction losses due to the electron hopping between Fe^{2+} and Fe^{3+} ions [29]. Fig. 3 indicates that resistivity of the samples decreases with the decrease in pH and hence conductivity increases. As the decrease in pH results increase in the grain size and decrease in grain boundaries. Thus conductivity increases and conduction losses increases. Dielectric loss ($\tan\delta$), dielectric constant (ε'), dc electrical resistivity (ρ) and drift mobility (μ_d) of samples of $SrFe_{12}O_{19}$ for different values of pH is given in Table 2.The dielectric loss factor (ε'') is calculated by using equation [32]

$$\varepsilon'' = \varepsilon' \tan\delta \quad (6)$$

The plot of dielectric loss factor (ε'') as a function of frequency for all samples is shown in Fig. 4(c). The trend is similar to dielectric loss ($\tan\delta$) as shown in Fig. 4(b). At lower frequencies, high dielectric loss factor (ε'') may be because of impurities, crystal defects and moisture. Hudson [33] has shown that the dielectric losses in ferrites are mainly because of conduction mechanism due to space charge polarization. As the frequency of the applied electric field increases, the charges could not follow the alternating field. As a result the polarization decreases and hence dielectric loss decreases. Fig. 4(c) also shows that at lower frequencies, dielectric losses factor (ε'') increases with the decrease in pH and becomes nearly uniform at higher frequencies. This is because of the similar reason as explained above in dielectric loss ($\tan\delta$). These results are in consistent with dc resistivity measurements shown in Fig. 3. As the decrease in pH results increase in the grain size and decrease in grain boundaries. Thus conductivity increases and conduction losses increases and hence dielectric loss factor (ε'') increases.

4. Conclusions

Strontium hexa-ferrite nano particles were prepared by co-precipitation method for different pH values. X-ray diffraction analysis showed that primary phase of strontium hexa-ferrite was decreased and secondary phase of α-Fe_2O_3 was increased with the decrease in pH. SEM micrographs indicated that particle size and its range also increased by decreasing pH. The dc electrical resistivity was decreased with the decrease in pH due to the increase in grain size. Dielectric constant was measured in the frequency range of 1 kHz to 3 MHz. Results showed that rate of decrease in dielectric constant were higher at low frequencies than at higher frequencies. This was due to the fact that electron exchange between Fe^{2+} and Fe^{3+} ions could not follow alternating electric field at higher frequencies. The dielectric constant was also decreased with the decrease in pH due to decrease in the grain boundaries and concentration of Fe^{2+} ions. Dielectric loss ($\tan\delta$) was also affected by pH. Graphs indicated that dielectric loss ($\tan\delta$) increased with the decrease in pH. The decrease in pH resulted in the increase in particle size and decrease in grain boundaries. The conduction losses were increased and hence dielectric losses were increased. The effect of pH on both dielectric constant and dielectric loss was prominent at lower frequencies and became nearly uniform at higher frequencies.

Acknowledgements

This work was financially supported by Higher Education Commission Pakistan through “Indigenous 5000 Scholarship Program” and “National Research Program for Universities (NRPU # 893)”. Mr. M.S. Awan is acknowledged for his cooperation.

References

[1] H. Kojima, in: E.P. Wohlfarth (Ed.), Ferromagnetic Materials, vol. 3, Amsterdam, 1982.
[2] E.J.W. Verwey, P.W. Haaijman, F.C. Romeyn, G.M. Van Oosterhout, Phil. Res. Rep. 5 (1950) 173.
[3] M. Goyot, J. Magn. Magn. Mater. 18 (1980) 925.
[4] N. Ponpandian, P. Balaya, A. Narayanasamy, J. Phys. Condens. Matter 14 (2002) 3221.
[5] G.K. Thompson, B.J. Evans, J. Appl. Phys. 73 (1993) 6295.
[6] P. Sharrock, IEEE Trans. Mag., MAG 25 (1989) 4374.
[7] F. Tabatabaie, M.H. Fathi, A. Saatchi, A. Ghasemi, J. Alloys Compd. 470 (2009) 332.
[8] H.J. Kwon, J.Y. Shin, T.H. Oh, J. Appl. Phys. 75 (1994) 6109.
[9] Y. Kotsuka, H. Yamazaki, IEEE Trans. Electromagn. Comat 42 (2000) 116.
[10] M.H. Sousa, F.A. Tourinho, J. Phys. Chem. B 105 (2001) 1168.
[11] S.R. Mekala, J. Ding, J. Alloys Compd. 296 (2000) 152.
[12] S.E. Jacobo, L. Civale, M.A. Blesa, J. Magn. Magn. Mater. 260 (2000) 37.
[13] Y.F. Lu, W.D. Song, Appl. Phys. Lett. 76 (2000) 490.
[14] M.N. Ashiq, M.J. Iqbal, I.H. Gul, J. Alloys Compd. 487 (2009) 341.
[15] J.C. Burtfoot, Ferroelectrics: An Introduction to the Physical Principles, Van Nostrand-Reinbold, London, 1967.
[16] J. Molla, M. Gonzalez, R. Villa, A. Ibara, J. Appl. Phys. 85 (1999) 1727.
[17] E.J.W. Verwey, J.H. De Boer, Rec. Trans. Chim. Des. Pays. Bas 55 (1936) 531.
[18] J.A. Rodriguez, M. Fernandez-Garcia, Synthesis, Properties and Applications of Oxide Nanomaterials, John Wiley & Sons Inc, New York, 2007.
[19] D. Segal, J. Mater. Chem. 7 (1997) 1297.
[20] A. Goldman, Modem Ferrite Technology, second edition, Springer Science + Business Media Inc., 2006.
[21] Q.Q. Fangb, H.W. Baob, D.M. Fangb, J.Z. Wangb, X.G. Lia, J. Magn. Magn. Mater. 278 (2004) 122.
[22] M.M. Hessien, M.M. Rashad, K. El-Barawy, J. Magn. Magn. Mater. 320 (2008) 336.
[23] B. Kaur, M. Bhat, F. Licci, R. Kumar, K.K. Bamzai, P.N. Kotru, J. Mater. Chem. Phys. 103 (2007) 255.
[24] A. Lakshman, P.S.V.S. Rao, B.P. Rao, K.H. Rao, J. Phys. D: Appl. Phys. 38 (2005) 673.
[25] J. Smit, H.P.J. Wijin, Ferrites, Wiley, New York, 1959.
[26] T. Abbas, M.U. Isalm, M.A. Chaudhry, J. Modern Phys. Lett. B 9 22 (1995) 1419.
[27] K.W. Wanger, Ann. Phys. 345 (1913) 817.
[28] M.J. Iqbal, M.N. Ashiq, J. Chem. Eng. 136 (2008) 383.
[29] L.B. Kong, Z.W. Li, G.Q. Lin, Y.B. Gan, J. Am. Ceram. 90 (7) (2007) 2104.
[30] N. Sivakumar, A. Narayanasamy, C.N. Chinnasamy, B. Jeyadevan, J. Phys. Condens. Matter 19 (2007) 386201.
[31] C.G. Koops, Phys. Rev. 83 (1951) 121.
[32] I.H. Gul, A. Maqsood, J. Alloys Compd. 465 (2008) 227–231.
[33] A.S. Hudson, Marconi Rev. 37 (1968) 43.